



# A streaming-potential-based microfluidic measurement of surface charge at immiscible liquid-liquid interface

Amer Alizadeh<sup>a,b,c,1</sup>, Yunfan Huang<sup>a,1</sup>, Fanli Liu<sup>a</sup>, Hirofumi Daiguji<sup>b</sup>, Moran Wang<sup>a,\*</sup>

<sup>a</sup> Department of Engineering Mechanics, Tsinghua University, Beijing, China

<sup>b</sup> Department of Mechanical Engineering, The University of Tokyo, Tokyo 113-8656, Japan

<sup>c</sup> Department of Chemical and Petroleum Engineering, Schulich School of Engineering, University of Calgary, Calgary, AB T2N 1N4 Canada

## ARTICLE INFO

### Keywords:

Immiscible liquid-liquid interface  
Surface charge  
Streaming potential experiment  
Electrical double layer

## ABSTRACT

Surface charging at immiscible liquid-liquid interface is essential to the emulsion stability, surfactant adsorption, and various engineering applications such as drug delivery and mineral flotation. However, droplet electrophoresis, as a widely-used electrokinetic method to measure the surface charge density, has various limitations in physical modeling and sample preparation. In this work, an alternative experimental method based on streaming potential setup is proposed. A Y-Y shaped microchannel was used to make a flat and stable liquid-liquid interface. The inner wall was coated with polymer to suppress the interference of the solid-liquid interfacial electrokinetics in the liquid-liquid one. The experimental setup was first verified by revisiting the aqueous solution-silicon surface charging, after which the surfactant-free decane-KCl solution interface charging was investigated. The negative surface charge at the decane-KCl solution interface is confirmed and found to increase when increasing the pH. This result is compatible with the probable charging mechanism that the acquired negative surface charge results from hydroxyl ion adsorption onto the interface. The proposed method enables the simplicity and flexibility for further side-by-side studies on the liquid-liquid interface charging mechanism and will inspire the quantitative macroscopic interfacial modeling for numerous scenarios, such as the droplet electrophoresis and interfacial electro-hydrodynamics.

## 1. Introduction

The spontaneous charging of the immiscible liquid-liquid interface has attracted much attention for its diverse implications from the basic issues on the emulsion stability, the hydrophobic effects, and multiphase electrohydrodynamics [1–3], to the various engineering applications including drug delivery in pharmaceutical industries, mineral flotation and hazardous substance separation in earth and environmental engineering, enhanced oil recovery such as low salinity waterflooding in petroleum engineering, capillary/microfluidic chip electrophoresis in biochemical analysis, and electrohydrodynamic 3D printing technology [4–8]. It has been demonstrated how the electrostatic interactions greatly influenced the stability of thin emulsion films with nonionic surfactants, and the strong hydrophobic attractions are usually accompanied by the repulsion forces originally due to the acquired charge at water-hydrophobic interfaces. In unconventional oil resources, since the interaction of the oil droplets with brine and rocks (such as the electrical

double layer repulsion between oil and rock) is of crucial importance, comprehensive understanding of the physical chemistry of the oil-water interface will enhance our ability for oil recovery [9,10]. Recently, a general trend of growing interest has been seen in the water-hydrophobic interfacial charging phenomena, such as contact electrification and electron transfer at water-hydrophobic interface [11, 12], surface adsorption of proteins and vehicles [13,14], and electrostatic and entropic interactions between particles at interface [15,16].

People have shown that the water-hydrophobic interface could be charged by introducing surfactants [17]. Surprisingly, for a surfactant-free oil-water interface, the single oil droplet in an aqueous solution is found to move from the cathode to the anode under an external electric field, indicating that this pristine interface is also charged [18]. In their landmark work, Marinova et al. [19] performed a series of electrophoresis experiments and theoretical evaluations and clarified that the oil-water interface is negatively charged. It is also observed that by increasing the pH of the aqueous solution, the

\* Corresponding author.

E-mail address: [mrwang@tsinghua.edu.cn](mailto:mrwang@tsinghua.edu.cn) (M. Wang).

<sup>1</sup> These authors contributed equally to this work.

electrophoresis mobility of the oil droplet will significantly increase, which indicates that the negative surface charging may originate from the physical adsorption of the hydroxyl ions at the interface released by the water molecules. Though it has been widely accepted that the water-hydrophobic interface is negatively charged over a large pH range (from 3–4 to 10–11), an intense long-lasting debate on the detailed interfacial charging mechanism and electrostatic structure is ongoing from 1935 to now [20–22]. In particular, though the effective charge of water-hydrophobic surfaces (in particular, the air–water interface) has been always a crucial parameter for electrochemistry, soft matter, and colloid science, its unambiguous measurement remains a challenge. Besides, a major challenge in the theoretical modeling and numerical simulation study of liquid phases is that unlike solids and vapor, no assumption of the detailed periodicity or homogeneity of their structure can be made, for which the molecular structure of the water-organic solvent interface has remained controversial [23,24].

Plenty of experiments have been implemented to explore the charging mechanism and electrostatic structure at the liquid-liquid interface, which can be divided into two categories: one is the qualitative characterization using vibrational spectrometry to detect the species at the interface (such as second-harmonic generation, sum-frequency generation, mass spectrometry, and X-ray photoelectron spectroscopy), while the other is the quantitative measurement with certain theoretical model to extract the surface charge density (such as potentiometric titration, surface tension measurement, double layer force measurement, electric capacity, and electroacoustic measurement). In this work, we will focus on the latter one, and more specifically, the electrokinetics-based (EK-based) method, which is probably the most widely-used method to characterize the magnitude of the surface charge. EK-based method focuses on the coupling flow of solution fluid and charged species due to the distributed ions around the charging interface, which includes various types of experimental setup, such as electroosmotic mobility, electrophoresis mobility, streaming potential/current measurement, and electroacoustic measurement. This kind of method is appreciable for almost any interface, such as solid/liquid, liquid/liquid, and gas/liquid interfaces, and is also quite easy to implement with relatively well-established theories. Compared to the other experimental methods for quantitative measurement, the EK-based method has the following advantages: (1) in EK modeling only the ion distribution structure around the interface (such as the electrical double layer (EDL) theory) is essential, which avoids the additional assumption on the detailed electrification mechanism at interface that should be already known before performing the experiment in potentiometric titration, electric capacity measurement, and surface tension measurement; (2) only macroscopic modeling with rather simple mathematical formulation (for the general cases) is needed, while for double layer force measurement the additional surface forces in the disjoining pressure term are required to be carefully treated; (3) only tangential transport along the charged interface is induced, which avoids the additional modeling of charge redistribution across the interface in the electric capacity measurement.

In respect of the water-hydrophobic interfacial electrokinetics, different types of the EK-based experiments have been chosen for different systems. For solid-state hydrophobic (solid-liquid interface), quite a lot of electroosmosis and streaming potential experiments have been implemented [25], while for liquid hydrophobic (immiscible liquid-liquid interface), only the electrophoresis method has been utilized regarding the surface charge measurement to the best of our knowledge [19,26–29] (see Table 2 for a comprehensive comparison). However, as elucidated in a recent review and indicated from the previous simulation [30,31], the droplet electrophoresis method suffers from various issues on both the experimental technique and theoretical modeling sides, especially at a high zeta potential. First, the slip velocity at the liquid-liquid interface cannot be ignored under an external electric field and the tangential transport of interface charge will lead to an additional effective surface conduction, which will increase the

inaccuracy of the measurement compared to the solid particle electrophoresis. Second, the charge redistribution around the interface due to the droplet deformation and the interface movement will modify the EDL polarization thus the extraction formulation of the interface charge density from the emulsion mobility. Third, the droplet size, polydispersity, and stability of the emulsions are strongly dependent on the surface charging density, which is also encountered in electroacoustics, making it hard to obtain a general relationship between the surface charge and various solution properties in a wide parameter range. Last but not least, the preparation process of emulsions used in the electrophoresis experiments requires special treatments to ensure high purity and low polydispersity of the emulsions, which may induce additional disturbing factors impacting the accuracy of measurements. The uncertainties above make the measurement of the liquid-liquid interfacial charge indeed an open question, and the previous results are meaningful only in the sense of magnitude to a certain degree.

In this work, we propose a novel experimental method using microfluidics with a streaming potential formulation to measure the surface charge at an immiscible liquid-liquid interface. Inspired by the design of the co-current flow pattern in microfluidic liquid-liquid extractors, we make a flat and stable interface between the two liquids based on a Y-Y shaped microchannel utilized for streaming potential measurement. This enables the access to both sides of the interface and the flexibility of side-by-side studies on the EDL properties for liquid-liquid interfaces with various solution properties. We also avoid the difficulties induced by the inaccuracy from droplet polydispersity due to sample preparation and complexity of physicochemical transport modeling at curved interfaces [30]. Besides, the microfluidic substrate is coated with polymers to suppress the zeta potential at the solid-liquid interface, which reduces its possible strong interference in the liquid-liquid interfacial electrokinetics [32,33]. This experimental setup is then utilized to measure the surface charge at decane-KCl solution interface as a preliminary application, whose results are compared with the previous experimental ones obtained by the other electrokinetic method and briefly discussed based on the magnitude of the results. To the best of our knowledge, our proposed methodology for the first time measures the liquid-liquid interfacial electrokinetics using the streaming potential method in microfluidics. Our work lays the foundation for further explorations and physical discussions on the charging mechanism at immiscible various liquid-liquid interfaces [34,35] and will promote the macroscopic interfacial modeling for the numerous application scenarios [36,37].

The article is organized as follows. In Section 2, the materials and methods of experimental setup are described in detail to highlight our innovative thoughts in this contribution. In Section 3, the results of the surface charge and the zeta potential at the decane-KCl solution interface from streaming potential measurement are presented and briefly discussed. The conclusions are summarized in Section 4.

## 2. Materials and methods

There are two major challenges when designing a streaming potential experiment including liquid-liquid interfacial electrokinetics. On the one hand, instability phenomena occurs at the liquid-liquid interfaces with non-zero shear stress between liquids of different viscosities due to the velocity mismatch (“Kelvin-Helmholtz instability”), vorticity mismatch (“Yih instability”) and normal pressure imbalance (“Saffman-Taylor instability”), which may lead to the chaotic interfacial flow prohibiting the steady formation which is required for a streaming-potential-based measurement. On the other hand, the surface charge density on microchannel walls may be comparable to the one at the liquid-liquid interface as confirmed in the previous studies [17,38], which will strongly interfere the measured electrokinetic streaming potential. In this regard, we manage to develop a flat and stable liquid-liquid interface by an extractor-like Y-Y shaped microchannel design with approximate co-directional entry for two liquid phases (as

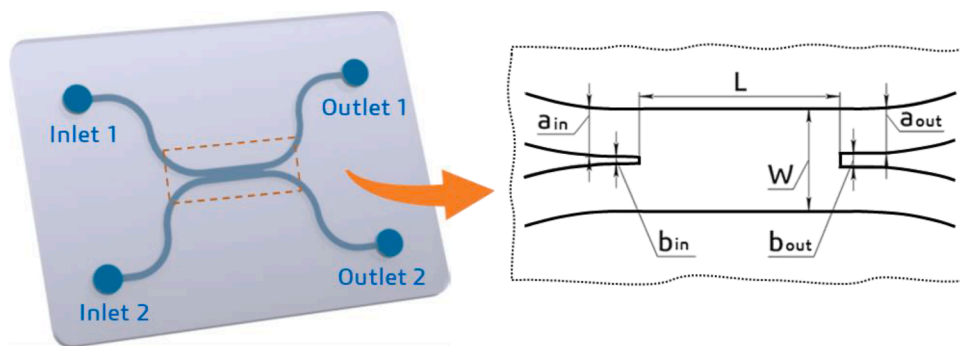


**Fig. 1.** The microfluidic chip with a Y-Y shaped microchannel designed for the present experimental study, which has two inlets and two outlets with depth  $H = 100 \mu\text{m}$ , width  $W = 1017 \mu\text{m}$ , and length  $L = 4200 \mu\text{m}$  for the middle part of the channel. The left-hand side channels are designed to separate by a thinner gap ( $b_{in} \approx 60 \mu\text{m}$ ) to suppress the inlet disturbance normal to the oil-aqueous solution interface, while the thickness of right-hand side gap is a little bigger ( $b_{out} \approx 120 \mu\text{m}$ ) to guarantee the interface formation and directing to their outlet reservoirs.

shown in Fig. 1) and perform an appropriate pressure control to ensure the zero shear stress condition at the interface approximately [39]. Besides, a synthesized polymer (PMSi) is used to coat the silicon microchannel wall, which suppresses the zeta potential at the silicon-aqueous solution interface to a great extent and relatively amplifies the effect of liquid-liquid interfacial electrokinetics.

In this work, two sets of streaming potential experiment were performed successively. Firstly, we measured the zeta potential of the designed silicon microchannel without coating by flowing a single-phase NaCl solution to compare our results with the electric quad layer (EQL) theoretical model as well as the previous experiments, and then repeated the process using a coated microchannel to verify the effectiveness of polymer coating on suppressing the zeta potential on the microchannel walls. Secondly, a flat and stable oil-water interface was made inside the coated silicon microchannel and surface charge at the oil-water interface was measured by streaming potential formation as an exemplar application of our novel application of the design.

In this section, the materials are first introduced. Then comes the detailed solution to the foregoing challenges. Specifically, the microfluidic design and the pressure controlling issue are illustrated in Section 2.2. while polymer coating technique is elucidated in Section 2.3.

## 2.1. Materials

Analytical reagent decane ( $\text{C}_{10}\text{H}_{22}$ ) (Maclin) is used as the oil phase with the purity of 98%. The viscosity of decane is  $920 \mu\text{Pa}\cdot\text{s}$  and the density is  $0.73 \text{ g/mL}$ . The decane (polarity index = 0.3 (Snyder)) as a non-polar liquid is an immiscible liquid into the water (polarity index = 9.0 (Snyder)) [40]. As a result, a sharp interface between the decane and water is expectable. Interfacial tension between our decane and deionized water sample is measured by Drop Shape Analyzer (DSA25, Krüss, Germany) for three times, the result showing  $49.105 \pm 0.397 \text{ mN/m}$ , in agreement with  $51 \pm 4 \text{ mN/m}$  in the previous literatures [41].

For the aqueous phase, two different kinds of solutions are used in different sets of experiments: (1) in the first set, NaCl (Maclin) solution is used to perform the verification of the zeta potential measurement on the microchannel walls. Different pH solutions are prepared by adding NaOH to the ultra-pure water. NaCl is added to the different pH solutions which gives solutions of 10 and 100 mM. The pH is measured by the METTLER TOLEDO and the solution electrical conductivity by EUTECH instruments CON 2700. (2) in the second set, KCl (Maclin)

solution is used as the aqueous phase. The pH of the KCl solution is adjusted by adding NaOH to the ultra-pure water. To study the impact of bulk ionic concentration, we make four different KCl solutions whose pH and concentration are shown in Table 1. Both the pH and the conductivity of the solution are measured three times to make sure about the repeatability of the measurements.

The microchannel is made of silicon and sealed by glass, which is coated by poly(MPC-co-MPTMSi) (referred to as PMSi) when measuring the streaming potential induced by the surface charge at liquid-liquid interface, where MPC and MPTMSi are the abbreviations of 2-methacryloyloxyethyl phosphorylcholine and 3-methacryloxypropyl trimethoxysilane, respectively. To be specific, MPC is a synthesized polymer utilized to make the internal surface of the microchannel more hydrophilic and suppress the zeta potential substantially [33], while MPTMSi incorporated in the polymers acts as the methacrylate silane-coupling unit, which is bound to the silicon substrate covalently ensuring the repeatability of the coated microchannel in electrokinetic measurements. To make the proper coating solution, liquid A which is known as PMSi91 with 0.2% (wt) ethanol solution is mixed with liquid B which is a catalyst-succinic acid ethanolic solution in a 10:1 (v/v) ratio.

The temperature of the laboratory is controlled at around  $24\text{--}25 \text{ }^\circ\text{C}$ .

## 2.2. Y-Y shaped microchannel design and driving pressure control

A Y-Y shaped microchannel with two inlets and two outlets is specially designed for making a flat and stable oil-water interface by injecting the oil and aqueous solution from different inlet ports, as shown in Fig. 1.

The pressure is controlled by FLUIGENT MFCS-EZ which has four-channel microfluidic flow control system, which could be controlled by the computer. By adjusting the pressure at decane and KCl solution reservoirs, the flow rates of the two liquid phases on the two sides of oil-water interface in the microchannel are maintained close to each other to ensure the approximate flat and stable interface in the second set of experiments, which will lead to an approximate zero shear stress at the interface and suppress the interfacial velocity and vorticity mismatch which eventually reduces the Kelvin-Helmholtz and Yih instability (see Fig. 4(a)).

Now we evaluate the pressure at both KCl solution and decane reservoirs to make the volume flux of the two phases approximately equal, i.e.,  $Q_w = Q_o$ , which is required to make the zero shear stress at the

**Table 1**

The charge density and zeta potential as well as the total volume number of assumed hydroxyl ions at the solution-oil interface obtained from measurements.

$(n_b \text{ (mM), pH})$	$n_b = 1 \text{ mM}$		$n_b = 10 \text{ mM}$	
	$\text{pH} = 8.90$	$\text{pH} = 4.56$	$\text{pH} = 8.90$	$\text{pH} = 9.70$
$\sigma \text{ (} \times 10^{-6} \text{ mC/cm}^2\text{)}$	$-12.53 \pm 0.41$	$-5.35 \pm 1.07$	$-7.29 \pm 0.13$	$-25.36 \pm 8.39$
$\zeta_{o-w} \text{ (mV)}$	$-10.42 \pm 0.34$	$-1.41 \pm 0.28$	$-1.92 \pm 0.03$	$-6.67 \pm 2.21$
$n_{\text{OH}^-, \text{ow}}$	3.28	1.40	1.91	6.65
$n_{\text{OH}^-, \text{b}}$	1.02	$4.67 \times 10^{-5}$	1.02	6.45

liquid-liquid interface. The relation between the volume flux and pressure drop is

$$Q_i \propto \alpha_{\text{geo}} \frac{\nabla P_i}{\mu_i}, \quad (i = w, o) \quad (1)$$

where the subscripts “w” and “o” denote the electrolyte solution and oil respectively,  $Q$  the net volume flux,  $\nabla P$  the pressure gradient, and  $\mu$  the viscosity,  $\alpha_{\text{geo}} \simeq \mathcal{A}^3/2\mathcal{P}^2$  is the geometric parameter with the perimeter  $\mathcal{P}$  and the area  $\mathcal{A}$  [42]. Since the width of the electrolyte solution and oil phase has been considered equal,  $\alpha_{\text{geo}}$  takes the same value for both the oil and water sides and thus

$$\frac{\nabla P_w}{\mu_w} = \frac{\nabla P_o}{\mu_o} \quad (2)$$

which gives a relation of interfacial compatibility to set the initial pressures at both KCl solution and oil reservoirs. Since the viscosities are known, we only need to set one pressure gradient (e.g., KCl solution side) and then the pressure gradient at the oil side would be obtained. Noticing that these pressure gradients are only the estimated ones, to make the oil-KCl solution interface in practice, we need to control the pressure gradients carefully in both oil and KCl solution reservoirs to make a stable interface at the middle of the microchannel.

Here we should mention that for very low bulk ion concentration, it would be hard to accurately measure the zeta potential since even dissolving a small amount of the  $\text{CO}_2$  could change the results significantly. To avoid any possibility of dissolving the  $\text{CO}_2$  in water and changing the pH of the solution, our experimental setup is isolated from the atmosphere by using closed inlets of both reservoirs and the microchannel ports and a 99% pure  $\text{N}_2$  is utilized to drive the solution from the pressurized reservoirs into the outlet ones. The 99% pure  $\text{N}_2$  is employed to provide pressure for channels of the FLUIGENT pressure controller. Using highly purified  $\text{N}_2$  makes sure that there would be less possibility of affecting the results by dissolving gasses like  $\text{CO}_2$  (Fig. 2).

### 2.3. Streaming potential measurement and polymer coating

The streaming potential is measured by KEITHLEY 6517B and Ag/AgCl electrode is used as the working electrode. By controlling the applied pressure, the steady-state streaming potential is achieved when the measured electric potential becomes approximately constant versus time.

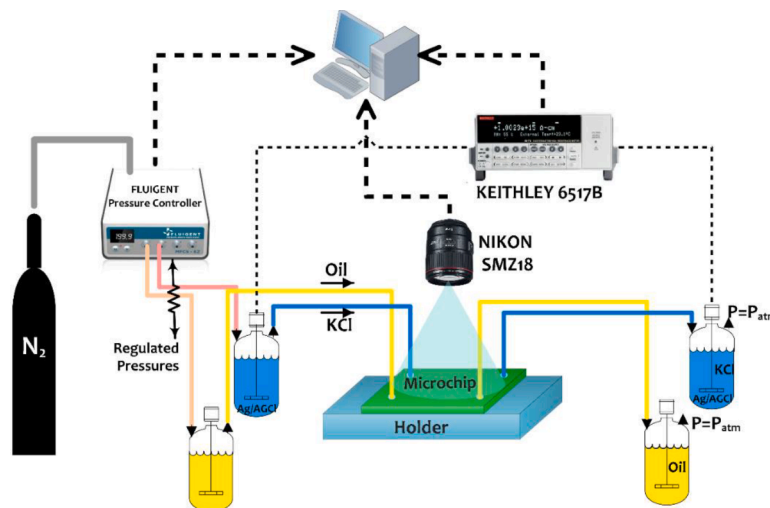


Fig. 2. The experimental setup for measuring the surface charge at the oil-water interface. Four reservoirs are connected to the four ports of the microchannel. We have used two reservoirs pressurized by an external pressure source. The solution flows from capillary tubes to the inlet of the microchannel, while the outlet bath is left to the atmospheric pressure. By adjusting the pressure gradient in the solution side, the streaming potential with the aid of the Ag/AgCl electrodes can be measured.

The coating procedure for the silicon microchannel is elucidated as follows. First, the working solution is prepared every time the coating procedure is performed. Second, the solution is injected into the microchannel by employing high enough pressure for the  $\text{N}_2$  to observe that the whole solution transfer from the input reservoir into the output one. We repeat this procedure for several minutes. Third, the 99%  $\text{N}_2$  is injected to evaporate the solvent from the microchannel at room temperature, after which the microchannel is put inside the heater at  $70^\circ\text{C}$  for 4 h. Finally, before using the silicon microchannel, it is recommended that the microchannel be filled with DI water to equilibrate the interfaces (Ishihara Laboratory, Department of Bioengineering, The University of Tokyo).

## 3. Results and discussions

### 3.1. Revisit of solution-silicon interfacial charging

In the first set of experiments, we employ the streaming potential experiment to measure the zeta potential at the aqueous solution-silicon interface to evaluate our capability of measuring and suppressing the zeta potential of the solid-liquid interface. By changing the pressure gradient, the zeta potential is obtained by measuring the slope of the electric potential-pressure gradient curve [43]

$$\zeta = -\frac{\mu K_0}{\varepsilon} \left( \frac{\Delta E_s}{\Delta P} \right) \quad (3)$$

where  $\mu$  denotes the fluid dynamic viscosity,  $K_0$  the bulk electrolyte solution conductivity, and  $\varepsilon$  the permittivity of the bulk electrolyte solution.

We measured the streaming potential for solution pH ranges from 4.50 to 9.70 and two bulk ion concentrations of 10 and 100 mM. Fig. 3 shows the comparison of the experimental results with the electric quad layer (EQL) model and other experiments [44–46]. To compare our experimental results with the EQL model, we employed the same parameters as we presented in our previous work [44,46]. Our zeta potential measurements increase by increasing the solution pH, while the increase of the bulk ion concentration has a decreasing effect on the zeta potential. One main reason in favor of this fact could be the surface dissociation. When increasing the pH, more  $\text{SiOH}$ 's dissociate to the  $\text{SiO}^-$  and  $\text{H}^+$  with more negatively charged surface sites developed. On the other hand, when the concentration of the bulk ion concentration

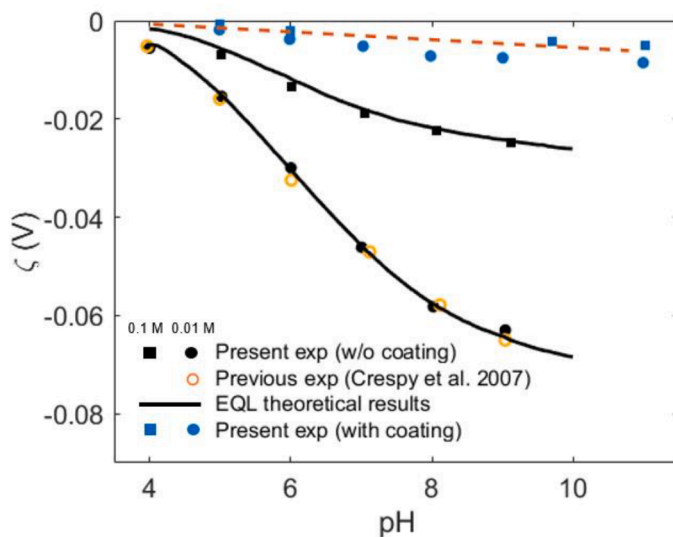


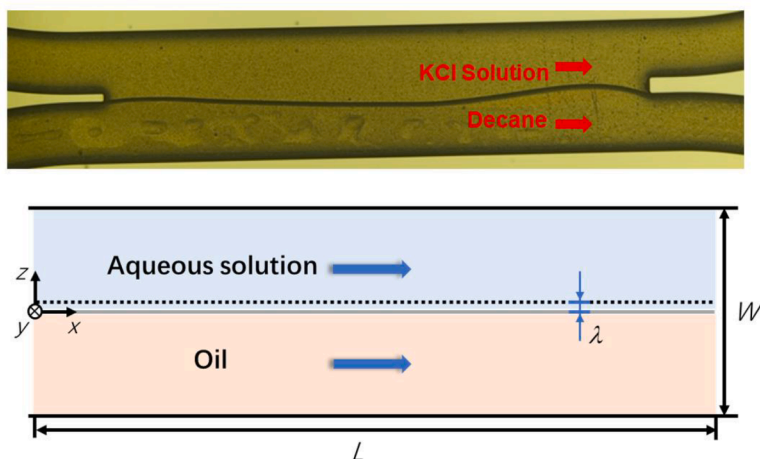
**Fig. 3.** The measured zeta potentials for different pH and two bulk ion concentrations ( $n_b = 0.01$  M; squares for  $n_b = 0.1$  M) in present experiments are denoted by the filled symbols, compared with the previous experimental data [45,46] denoted by the orange circles and the EQL modeling results [44] denoted by the solid curves. For the third bulk ionic concentration ( $n_b = 0.001$  M) only the EQL prediction is presented. Suppressing of the measured zeta potential after coating with PMSi (blue filled symbols) compared to the one before coating (black filled symbols) indicates that the microchannel has been coated successfully (red dashed line: the fitting curve). The relative errors of the present experimental results are within 5%.

increases, more surface sites will get counter-ions as SiOM. Here we should mention that for very low bulk ion concentration, it would be hard to accurately measure the zeta potential since even dissolving a small amount of the  $\text{CO}_2$  could change the results significantly.

It is shown that our method to measure the zeta potential could be reliably validated by the theoretical models as well as other experimental studies. From our zeta potential measurement results after coating, it is indicated that our coating was successful, and the zeta potential was suppressed up to 70–80%.

### 3.2. Results of the oil-water interfacial charging

Given the flat and stable oil-water interface shown in Fig. 4, a streaming potential measurement versus the pressure gradient on the water side is then performed and the dependence of surface charge density on the pH and bulk ionic concentration is studied. Fig. 4 (Top)



shows the interface of the decane-water that will be employed to measure the interfacial surface charge. It is worth pointing out that some water droplets have been trapped in the decane side of the interface which is due to pumping water firstly and then the decane. In this way, we can simply change the pressure on the oil side to make a stable interface. To avoid any impact from those droplets on our measurements, we make sure that the streaming potential measurements have been kept for several minutes and tried our measurements at least three times. The good repeatability of the measured streaming potential guaranteed that those water droplets have not significant impact on the decane-water interface as a result the acquired surface charge. Fig. 4 (Bottom) depicts a schematic illustration of the interface and the dimensions of the microchannel for theoretical modeling.

The surface density of charge acquired at the oil-water interface can be obtained by

$$\sigma = -\frac{6W\mu_w K_{w,0}}{H^2} \left( \frac{\Delta E_s}{\Delta P} \right) \quad (4)$$

where  $K_{w,0}$  denotes the solution bulk conductivity,  $H$  the depth of the microchannel at the middle part, and  $\Delta E_s/\Delta P$  represents the slope of the streaming potential gradient versus the pressure gradient. As for the zeta potential, we have

$$\zeta_{o-w} = \frac{\sigma}{\epsilon\kappa} \quad (5)$$

where  $\kappa = 1/\lambda$  denotes the inverse of the Debye length, and  $\epsilon = 6.95 \times 10^{-10}$  F/m the electrical permittivity of the KCl solution. For details of the theoretical derivation, see Appendix A. Here we only mention the most important assumption that influence of surface charge at the microchannel walls on the streaming potential can be neglected. Though it will be seen from the result that the liquid-liquid zeta potential is at the same scale as the suppressed solid-liquid ones, the influence of the latter on the streaming potential is still quite limited due to its relatively low velocity nearby. In fact, from careful calculation, the contribution of the solid-liquid surface charging to the total streaming potential is about 1–3%, which ensures the accuracy of our measurement.

The detailed experimental data is illustrated in Fig. 5. The acquired surface charge and zeta potential at oil-water interface by considering the impact of the solution pH and bulk ionic concentration are obtained from our streaming potential measurements, as shown in Table 1.

### 3.3. Discussions on the oil-water interfacial electrokinetics

As shown in Table 1, it is found that the surface charge at the decane-KCl solution interface is negative, and the acquired surface charge

**Fig. 4.** Top: The interface of the decane (the lower part) and KCl solution (the upper part) in the streaming potential measurement experiment. It is seen that there are some water droplets in the decane, although this will not influence the flow of the water/decane interface significantly. Bottom: A schematic of the quasi-planar interface of the decane-KCl solution along the microchannel. The microchannel is designed in a way that the depth of the microchannel is much less than its width ( $H \ll W$ ). The characteristic thickness of the EDL at the solution side could be evaluated by the Debye length  $\lambda = \sqrt{\epsilon k_B T / 2e^2 n_b}$ , where  $n_b$  and  $\epsilon$  are the bulk ionic concentration and the electrical permittivity of the bulk electrolyte solution, respectively.

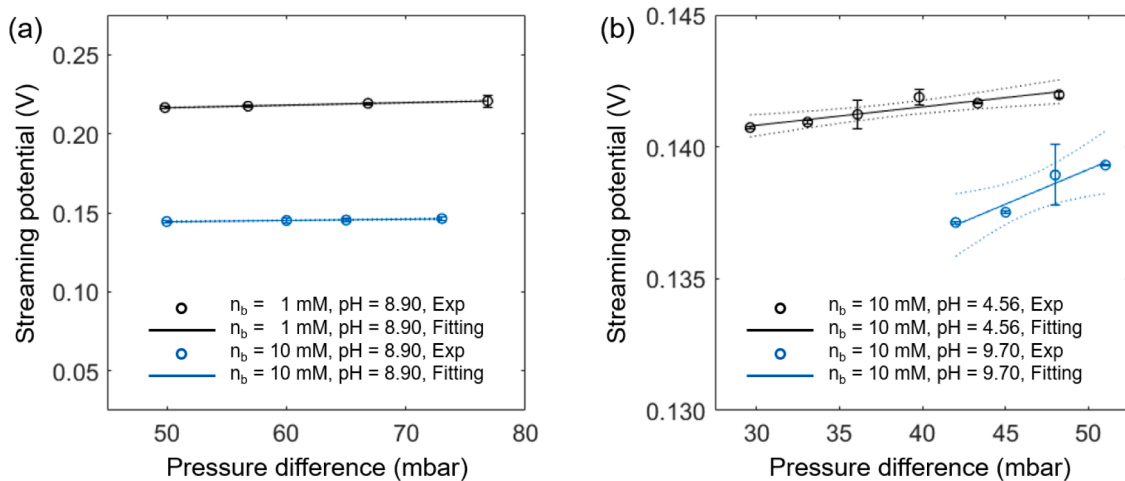


**Fig. 5.** The streaming potential as a function of the applied pressure gradient for (a)  $n_b = 1$  mM and 10 mM with pH = 8.90 and (b) pH = 4.56, 9.70 with  $n_b = 10$  mM. Dash lines represent the 95% confidence lines in the linear regression. The measured solution conductivities are  $\sigma_{w,0} = 0.1415$  S/m for  $(n_b$  (mM), pH) = (1, 8.90);  $\sigma_{w,0} = 0.1445$  S/m for  $(n_b$  (mM), pH) = (10, 8.90);  $\sigma_{w,0} = 0.1414$  S/m for  $(n_b$  (mM), pH) = (10, 4.56) and (10, 9.70).

increases significantly by increasing the pH (from pH = 4.56 to 9.70) of the solution, which indicates that the negative interfacial charging may be ascribed to the physical adsorption of  $\text{OH}^-$  at the KCl solution-decane interfaces [58]. It should be noted that the alternative charging mechanism may exist, such as the  $\text{H}^+$  adsorption, chloride ion adsorption, and carbonate adsorption [21], while the related discussion is beyond the scope of this manuscript. Regarding the impact of the solution bulk ionic strength ( $n_b$ ), Fig. 5(a) elucidates that the bulk ionic strength can also impact the surface charge and zeta potential at surfactant-free oil-water interface significantly.

Assuming that the adsorption of the hydroxyl ion is responsible for the acquired negative surface charge at the neat oil-water interface, the total number of hydroxyl ions ( $\text{OH}^-$ ) at the interface is  $n_{\text{OH}^-, \text{ow}} = \sigma LH / e$  and the total number of available hydroxyl ions in the microchannel is  $n_{\text{OH}^-, \text{b}} = 10^{3-(14-\text{pH})} N_A WLH / 2$ . Here,  $e = 1.602 \times 10^{-19}$  C is the charge of a single electron, pH is the bulk value, and  $N_A = 6.022 \times 10^{23} \text{ mol}^{-1}$  the Avogadro constant. Comparing the total interfacial hydroxyl ions  $n_{\text{OH}^-, \text{ow}}$  with the total available bulk hydroxyl ions  $n_{\text{OH}^-, \text{b}}$ , it is

surprisingly found that  $n_{\text{OH}^-, \text{ow}} \geq n_{\text{OH}^-, \text{b}}$  at pH = 4.56. This indicates the dramatic difference between the pH of aqueous solution in the bulk region and around the water-hydrophobic interfaces, which has been denoted by several previous papers [20,22].

Table 2 summarizes the previous experimental results obtained by electrokinetic methods after a careful literature review. As elucidated in the introduction part, the previous methods suffer from various forms of difficulties such as oversimplification of slip velocity and/or charge redistribution, strong dependence on colloid stability, and sensitivity in the preparation process, which makes the measurement of the liquid-liquid interfacial charging indeed an open problem. Thus, in this work as a prospective study, we mainly focus on the novel methodology of this streaming potential technique on liquid-liquid interfacial electrokinetics which avoids the physical and technical complexities above, and the results in Table 2 are provided for a preliminary comparison. The further systematic results of the dependence of surface charge on the solution properties on both sides with/without the presence of the surfactants will be covered in future studies.

**Table 2**

Electrokinetic property results of water-hydrophobic interface obtained by electrokinetic methods<sup>1</sup>.

Author	Year	Method	Non-polar phase	Polar phase	Average diam ( $\mu\text{m}$ )	$n_b$ (mM)	pH	$\sigma$ ( $\times [-10^{-6} \text{ mC/cm}^2]$ )	Modeling	$\zeta$ ( $\times [-1 \text{ mV}]$ )
Current work	2022	SP	$\text{C}_{10}$	KCl	–	1, 10	4.57–9.70	5–23	–	1–15
Parreira [47]	1961	SP	paraffin (s)	NaX	1000	$10^{-2}$ –10	5.8	0–1	–	10–40
Stachurski [26]	1985	EP	$\text{C}_9$ – $\text{C}_{16}$	NaCl	3–8	1	4–12	–	SMO [48]	20–90
Dunstan [49]	1992	EP	$\text{C}_{22}$ (s)	KCl	0.5	$10^{-3}$ – $10^2$	–	0–200	OBW [50]	0–75
Dunstan [51]	1993	EO	$\text{C}_{22}$ (s)	KCl	–	$10^{-3}$ – $10^2$	–	0–200	SMO	30–100
Barchini [17]	1996	EP	silicon oil	–	0.25–0.50	3–7	–	100–300 <sup>2</sup>	OBW	50–250
Marinova [19]	1996	EP	xylene	NaCl	0.1–1	$10^{-2}$ –10	4–9	–	SMO	20–80
Stachurski [52]	1996	EP	$\text{C}_6$ – $\text{C}_{16}$	NaCl	3–8	1	4–12	–	SMO	20–90
Jablonski [53]	1999	EP	$\text{C}_{18}$	NaCl	0.3	1–100	4–10	0–60,000 <sup>3</sup>	–	–
Yang [27]	2000	EP	$\text{C}_{16}$	NaCl	0.78	$10^{-3}$ –10	–	–	OBW	20–130
Zimmerman [54]	2001	SP	Teflon AF (s)	KCl	–	$10^{-3}$ – $10^2$	–	–	SCM	20–100
Beattie [38, 55]	2004	EA	$\text{C}_{16}$	NaX	0.4–0.9	0.4	9	5000	–	40–130
Franks [56]	2005	EA	$\text{C}_{16}$	AX	–	0.1–10	9	5000	–	30–70
Creux [28]	2009	EP/EA	$\text{C}_8$ – $\text{C}_{22}$	ACl	1000/0.5	$10^{-3}$	4–9	–	SWD [57]	20–90
Roger [29]	2012	EP	$\text{C}_{16}$	NaCl	0.17	1	4–11	545 <sup>4</sup>	OBW	–

<sup>1</sup> SP: streaming potential method; EP: oil-in-water electrophoresis method; EA: electroacoustics method.  $\text{C}_n$  denotes the  $n$ -alkanes, and “(s)” means the solid phase. Only results for monovalent are included;  $\text{A}^+ = \{\text{Li}^+, \text{Na}^+, \text{K}^+, \text{Cs}^+\}$ ;  $\text{X}^- = \{\text{Cl}^-, \text{Br}^-, \text{F}^-, \text{SCN}^-, \text{IO}_3^-, \text{ClO}_4^-\}$ . SMO: Smoluchowski’s formulation; OBW: O’Brien and White’s formulation; SCM: surface conductance modification; SWD: Sherwood’s formulation. All the listed experiments were done under room temperatures (22–25 °C).

<sup>2</sup> The excess surface charge is considered to arise from adsorbed ionic surfactant-sodium dodecyl sulfate (SDS).

<sup>3</sup> The excess surface charge is considered as the result of ionization of carboxyl groups of stearic acid adsorbed on the octadecane particle.

<sup>4</sup> The result is for 99.8% pure hexadecane, whose surface charge density is much less than the 99% pure one.

As shown in Table 2, our experimental results of zeta potential and surface charge density have roughly the same scale as or one order of magnitude lower than the previous EK-based experimental studies. From a more careful comparison with the previous experiments within the pH range of 4–10 and bulk ion concentration range of 1–10 mM and using the same salts (i.e., KCl) [49], it is seen that our results are slightly smaller, which is considered to result from the additional surface conduction and indicates one of the major disadvantages of the previous electrophoresis methods. As suggested, the increase in the cavity formation energy cost at higher ionic strengths also causes lower solute partitioning at the liquid-liquid interface (“salting-out” effect), which can also result in the reduction of the absolute value of the zeta potential at higher KCl concentrations. However, our result of surface charge density is only 1% of the previous electroacoustic measurement, which may be ascribed to the following reasons. First, the electroacoustic measurement needs the assumption of the droplet size distribution such as its obeying the log-normal function, which may differ much between different samplings and unavoidably induce the difficulty in repeatability. Second, generally speaking, in the experimental setup of our streaming potential method, though the electrode polarization and steady inlet/outlet effect have been tried to eliminate which has been verified through the solid-liquid streaming potential experimental benchmark, there still can be several unsteady effects which leads to some nonlinear errors (see the relatively large error bar in the Fig. 5(b) for example). Third, the interfacial polarization in the oil phase due to overcharging or specific adsorption may also give rise to an additional surface conduction with the electric double layer in the aqueous phase which is not considered in our physical model.

It is noteworthy that besides the unresolved question of the charging mechanism and ion distribution at liquid-liquid interface, the complete physical (or at least, effective) description of the liquid-liquid interfacial electrokinetics is still an open problem even for “the simplest system” such as droplet electrophoresis. Recent theoretical and numerical studies have explored the droplet electrophoresis coupled the electrokinetic formulation with the electrohydrodynamic model [36,59], which sheds light on the novel understanding of the electrodynamic of moving bodies with liquid-liquid interfaces between strong electrolyte solutions and leaky dielectrics, as well as related electrokinetic and colloidal transport phenomena. As elucidated in the literature, coupling of experiments and simulations is pivotal to mitigate methodological shortcomings and address open problems pertaining to charged interfaces [24]. Our experimental platform provides a simple and repeatable setup, which lays the experimental foundation for the quantitative modeling and simulation works in the future.

#### 4. Conclusion

We propose an experimental method to investigate the surface charging at both sides of the liquid-liquid interface based on a streaming potential setup. The Y-Y shaped microchannel design with polymer coating treatment is firstly introduced to the streaming-potential-based microfluidic measurement of surface charge at liquid-liquid interface [39,60], which tackles the limitations in the droplet electrophoresis mechanism and avoids the additional emulsion preparation process

#### Appendix A. Derivation of the liquid-liquid interface charge calculation formula ignoring solid-liquid interfacial electrokinetics

The following assumptions are made in this derivation: (1) neglected influence of surface charge at the microchannel walls on the streaming potential; (2) thickness of water-oil EDL in the water side is thin enough ( $\lambda \ll H, W$ ); (3) zeta potential of water-oil interface in the water side is not large (Debye-Hückel approximation, i.e.,  $\zeta < 25.4$  mV at room temperature); (4) charges inside the water-oil EDL in the water side are electrically neutralized by the surface charge; (5) flow in the aqueous solution side is approximately uniform in the  $z$  direction near the liquid-liquid interface region since  $H \ll W$ ; (6) water-oil interface is approximately flat with zero shear stress; (7) neglected influence of streaming potential on the fluid flow, indicating that the primary electro-viscous effect is ignored; (8) neglected surface conduction inside the water-oil EDL (both the diffuse layer and Stern layer) in the water side; (9) conducting current is totally induced by the streaming potential in the water side, supposing that the influence of possible

compared to the electrophoresis measurement [30,34].

The negative surface charge at the decane-KCl solution interface is confirmed, which is found to increase with the increasing pH of electrolyte solution and decreasing bulk concentration of indifferent ions. This result is compatible with the probable charging mechanism that the acquired negative surface charge results from hydroxyl ion adsorption onto the interface. The zeta potential and surface charge density are found to be at the same scale as the previous EK-based experimental studies. The detailed quantitative differences of may result from the surface conduction effect which is one of the disadvantages of the previous electrophoresis methods, and may also arise from the salting-out effect and/or the interfacial polarization due to specific adsorption effect of ions other than the hydroxyl ones.

As a prospective study, the present experimental setup can be easily extended to further studies on the dependence of surface charge on the solution properties on both sides with/without the presence of the surfactants. Owing to the simplicity and flexibility, our proposed experimental platform, combined with further theoretical and numerical studies, will promote the in-depth physical understanding of the liquid-liquid interfacial electrokinetics, electrodynamic of moving bodies with liquid-liquid interfaces, and related colloid transport phenomena, such as ion distribution around air-water interface [37,61] and droplet electrophoresis [30,36,59].

#### CRedit authorship contribution statement

**Amer Alizadeh:** Investigation, Validation, Writing – original draft. **Yunfan Huang:** Validation, Investigation, Writing – original draft. **Fanli Liu:** Validation. **Hirofumi Daiguji:** Writing – review & editing. **Moran Wang:** Conceptualization, Supervision, Writing – review & editing, Project administration.

#### Declaration of Competing Interest

The authors declare that they have no known competing financial interests or personal relationships that could have appeared to influence the work reported in this paper.

#### Data availability

No data was used for the research described in the article.

#### Acknowledgments

AA is very thankful to supports from Ishihara Laboratory, the University of Tokyo and fruitful discussions with Prof. Kazuhiko Ishihara, and Dr. Kyoko Fukazawa. The authors would like to thank the anonymous referee who provided useful and detailed comments on the manuscript. This work was financially supported by the National Natural Science Foundation of China (No. 12272207, U1837602, 51676107, 51176089), the National Key R&D Program of China (No. 2019YFA0708704) and the UTokyo-Tsinghua Collaborative Research Fund.

streaming potential in the oil side is neglected. Note that among those assumptions, (1)(2)(3)(5)(6)(7) could be easily verified according to the experimental condition and zeta potential results, while (4)(8)(9) are the modeling assumptions related to the unresolved physical mechanism.

We start from the Navier-Stokes equations for the aqueous solution side

$$0 = -\frac{dp_w}{dx} + \mu_w \frac{\partial^2 u_w}{\partial y^2} \quad (A1)$$

where  $u_w$  is the KCl solution flow velocity and  $p_w$  is the flow pressure. Integrating Eq. (A1), the parabolic velocity profile in the water side is simply obtained as

$$u_w(y) = \frac{-\nabla p_w}{2\mu_w} y(H-y) \quad (A2)$$

with  $\nabla p_w = (p_{out} - p_{in})/L \equiv -P/L$ . The streaming current is written as

$$I_{str} = \int u_w(y) \rho_e(z) dy dz \quad (A3)$$

Notice that the definition of the surface charge at the oil-water interface is

$$Q = - \int_0^{\infty} \rho_e(z) dz \quad (A4)$$

we can then perform the integration in Eq. (A3) by substituting Eqs. (A2) and (A4) which gives rise to

$$I_{str} = \frac{-P}{L} \frac{QH^3}{12\mu_w} \quad (A5)$$

On the other hand, the conducting current owing to the accumulation of the counter-ions in one end of the microchannel is obtained by

$$I_{cond} = (-\nabla\phi) K_{w,0} \frac{HW}{2} = \frac{-E_s}{L} K_{w,0} \frac{HW}{2} \quad (A6)$$

where  $\nabla\phi_w = (\phi_{out} - \phi_{in})/L \equiv E_s/L$ ;  $K_{w,0}$  and  $E_s$  denote the solution bulk conductivity and the measured streaming potential, respectively. From the current balance in the water side ( $I_{str} + I_{cond} = 0$ ), the relation for the surface charge at the oil-water interface is established [see Eq. (3)].

Considering the aqueous solution part of the microchannel as a channel with dissimilar surface charges, one can obtain the zeta potential of the oil-water interface in the water side as [62]

$$\zeta_{o-w} = \frac{\sigma}{2\epsilon\kappa} \left( \frac{1}{\tanh\left(\frac{\kappa h}{2}\right)} + \tanh\left(\frac{\kappa h}{2}\right) \right) \quad (A7)$$

For the non-overlapped EDL regimes (i.e.,  $\kappa h/2 > 2.8$ ) which yields  $\tanh(\kappa h/2) \approx 1$ , this results in the relation between zeta potential and surface charge at the oil-water interface [see Eq. (4)].

## References

- [1] Ghasemi E, Bararnia H, Soleimanikutanaei S, Lin CX. Direct numerical simulation and analytical modeling of electrically induced multiphase flow. *Int J Mech Sci* 2018;142-143:397-406.
- [2] Kronberg B. The hydrophobic effect. *Curr Opin Colloid Interface Sci* 2016;22:14-22.
- [3] Mueller H. The electrokinetic potential and the stability of colloids. *J Phys Chem* 1935;39:743-8.
- [4] Idrees H, Zaidi SZ, Sabir A, Khan RU, Zhang X, Hassan S-u. A review of biodegradable natural polymer-based nanoparticles for drug delivery applications. *Nanomaterials* 2020;10.
- [5] Liu F, Wang M. Review of low salinity waterflooding mechanisms: wettability alteration and its impact on oil recovery. *Fuel* 2020;267:117112.
- [6] Ramos-Payan M, Ocana-Gonzalez JA, Fernandez-Torres RM, Llobera A, Bello-Lopez MA. Recent trends in capillary electrophoresis for complex samples analysis: a review. *Electrophoresis* 2018;39:111-25.
- [7] Cañizares P, Martínez F, Lobato J, Rodrigo MA. Break-up of oil-in-water emulsions by electrochemical techniques. *J Hazard Mater* 2007;145:233-40.
- [8] Mohammadi K, Movahhedy MR, Khodaygan S. Colloidal particle reaction and aggregation control in the electrohydrodynamic 3D printing technology. *Int J Mech Sci* 2021;195:106222.
- [9] Tian H, Wang M. Electrokinetic mechanism of wettability alternation at oil-water-rock interface. *Surf Sci Rep* 2017;72:369-91.
- [10] Liu F, Wang M. Wettability effects on mobilization of ganglia during displacement. *Int J Mech Sci* 2022;215:106933.
- [11] Nauruzbayeva J, Sun Z, Gallo A, Ibrahim M, Santamarina JC, Mishra H. Electrification at water-hydrophobe interfaces. *Nat Commun* 2020;11:5285.
- [12] Zhao X, Lu X, Zheng Q, Fang L, Zheng L, Chen X, Wang ZL. Studying of contact electrification and electron transfer at liquid-liquid interface. *Nano Energy* 2021;87:106191.
- [13] Dickinson E. Adsorbed protein layers at fluid interfaces: interactions, structure and surface rheology. *Colloid Surf B-Biointerfaces* 1999;15:161-76.
- [14] Masschaele K, Park BJ, Furst EM, Fransaeer J, Vermant J. Finite ion-size effects dominate the interaction between charged colloidal particles at an oil-water interface. *Phys Rev Lett* 2010;105:4.
- [15] Aveyard R, Binks BP, Clint JH, Fletcher PDI, Horozov TS, Neumann B, Paunov VN, Annesley J, Botchway SW, Nees D, Parker AW, Ward AD, Burgess AN. Measurement of long-range repulsive forces between charged particles at an oil-water interface. *Phys Rev Lett* 2002;88.
- [16] Leunissen ME, van Blaaderen A, Hollingsworth AD, Sullivan MT, Chaikin PM. Electrostatics at the oil-water interface, stability, and order in emulsions and colloids. *Proc Natl Acad Sci* 2007;104:2585.
- [17] Barchini R, Saville D. Electrokinetic properties of surfactant-stabilized oil droplets. *Langmuir* 1996;12:1442-5.
- [18] Caruthers JC. The electrophoresis of certain hydrocarbons and their simple derivatives as a function of pH. *Trans Faraday Soc* 1938;34:300.
- [19] Marinova KG, Alargova RG, Denkov ND, Velev OD, Petsev DN, Ivanov IB, Borwankar RP. Charging of oil-water interfaces due to spontaneous adsorption of hydroxyl ions. *Langmuir* 1996;12:2045-51.
- [20] Björneholm O, Hansen MH, Hodgson A, Liu L-M, Limmer DT, Michaelides A, Pedevilla P, Rossmel J, Shen H, Tocci G. Water at interfaces. *Chem Rev* 2016;116:7698-726.

- [21] Yan X, Delgado M, Aubry J, Gribelin O, Stocco A, Boisson-Da Cruz F, Bernard J, Ganachaud F. Central role of bicarbonate anions in charging water/hydrophobic interfaces. *J Phys Chem Lett* 2018;9:96–103.
- [22] Vácha R, Buch V, Milet A, Devlin JP, Jungwirth P. Autoionization at the surface of neat water: is the top layer pH neutral, basic, or acidic? *Phys Chem Chem Phys* 2007;9:4736–47.
- [23] Gschwend GC, Olaya A, Peljo P, Girault HH. Structure and reactivity of the polarised liquid–liquid interface: what we know and what we do not. *Curr Opin Electrochem* 2020;19:137–43.
- [24] Liggieri L, Miller R. Combined surface analysis methods. *Curr Opin Colloid Interface Sci* 2018;37:A1–3.
- [25] Kirby BJ, Hasselbrink Jr EF. Zeta potential of microfluidic substrates: 2. Data for polymers. *Electrophoresis* 2004;25:203–13.
- [26] Stachurski J, Michałek M. The zeta potential of emulsion droplets of the aliphatic hydrocarbons in aqueous solutions. *Colloids Surf* 1985;15:255–9.
- [27] Yang B, Matsumura H, Kise H, Furusawa K. Aggregation behavior of hexadecane emulsions induced by egg yolk PC vesicles. *Langmuir* 2000;16:3160–4.
- [28] Creux P, Lachaise J, Graciaa A, Beattie JK, Djerdjev AM. Strong specific hydroxide ion binding at the pristine oil/water and air/water interfaces. *J Phys Chem B* 2009;113:14146–50.
- [29] Roger K, Cabane B. Why are hydrophobic/water interfaces negatively charged? *Angew Chem-Int Edit* 2012;51:5625–8.
- [30] Rashidi M, Zargartalebi M, Benneker AM. Mechanistic studies of droplet electrophoresis: a review. *Electrophoresis* 2021;42:869–80.
- [31] Li M, Li D. Redistribution of mobile surface charges of an oil droplet in water in applied electric field. *Adv. Colloid Interface Sci.* 2016;236:142–51.
- [32] Lappan U, Buchhammer HM, Lunkwitz K. Surface modification of poly(tetrafluoroethylene) by plasma pretreatment and adsorption of polyelectrolytes. *Polymer* 1999;40:4087–91 (Guildf).
- [33] Sibarani J, Takai M, Ishihara K. Surface modification on microfluidic devices with 2-methacryloyloxyethyl phosphorylcholine polymers for reducing unfavorable protein adsorption. *Colloids Surf B* 2007;54:88–93.
- [34] Uematsu Y. Electrification of water interface. *J Phys Condens Matter* 2021;33:423001.
- [35] Bazant MZ. Editorial Overview: fundamental and Theoretical Electrochemistry: advances in the theory of electrochemical interfaces. *Curr Opin Electrochem* 2019;13:A1–4.
- [36] Schnitzer O, Yariv E. The Taylor–Melcher leaky dielectric model as a macroscale electrokinetic description. *J Fluid Mech* 2015;773:1–33.
- [37] Dryfe RAW. The electrified liquid–liquid interface. *Adv Chem Phys* 2009;141:153–215.
- [38] Beattie JK, Djerdjev AM. The pristine oil/water interface: surfactant-free hydroxide-charged emulsions. *Angew Chem-Int Edit* 2004;43:3568–71.
- [39] Maurice A, Theisen J, Gabriel J-CP. Microfluidic lab-on-chip advances for liquid–liquid extraction process studies. *Curr Opin Colloid Interface Sci* 2020;46:20–35.
- [40] Snyder LR. Classification of the solvent properties of common liquids. *J Chromatogr A* 1974;92:223–30.
- [41] Sayed AM, Olesen KB, Alkahala AS, Sølling TI, Alyafei N. The effect of organic acids and salinity on the interfacial tension of n-decane/water systems. *J Pet Sci Eng* 2019;173:1047–52.
- [42] Bruus H. Theoretical microfluidics. Oxford: Oxford University Press; 2008.
- [43] Robert RHO, Hunter J, Rowell RL. Zeta potential in colloid science. principles and applications. Academic Press; 1981.
- [44] Alizadeh A, Wang M. Flexibility of inactive electrokinetic layer at charged solid-liquid interface in response to bulk ion concentration. *J Colloid Interface Sci* 2019;534:195–204.
- [45] Crespy A, Boleve A, Revil A. Influence of the Dukhin and Reynolds numbers on the apparent zeta potential of granular porous media. *J Colloid Interface Sci* 2007;305:188–94.
- [46] Wang M, Revil A. Electrochemical charge of silica surfaces at high ionic strength in narrow channels. *J Colloid Interface Sci* 2010;343:381–6.
- [47] Parreira H, Schulman JH. Streaming potential measurements on paraffin wax. ACS Publications; 1961.
- [48] Smoluchowski Mv. Contribution to the theory of electro-osmosis and related phenomena. *Bull Int Acad Sci Cracovie* 1903;3:184–99.
- [49] Dunstan DE, Saville D. Electrophoretic mobility of colloidal alkane particles in electrolyte solutions. *J Chem Soc Faraday Trans* 1992;88:2031–3.
- [50] O'Brien RW, White LR. Electrophoretic mobility of a spherical colloidal particle. *J Chem Soc Faraday Trans* 2 1978;74:1607–26.
- [51] Dunstan DE, Saville D. Electrokinetic potential of the alkane/aqueous electrolyte interface. *J Chem Soc Faraday Trans* 1993;89:527–9.
- [52] Stachurski J, Michalek M. The effect of the zeta potential on the stability of a non-polar oil-in-water emulsion. *J Colloid Interface Sci* 1996;184:433–6.
- [53] Jabłoński J, Janusz W, Szczypa J. Adsorption properties of the stearic acid-octadecane particles in aqueous solutions. *J Dispers Sci Technol* 1999;20:165–75.
- [54] Zimmermann R, Dukhin S, Werner C. Electrokinetic measurements reveal interfacial charge at polymer films caused by simple electrolyte ions. *J Phys Chem B* 2001.
- [55] Beattie JK, Djerdjev AM, Franks GV, Warr GG. Dipolar anions are not preferentially attracted to the oil/water interface. *J Phys Chem B* 2005;109:15675–6.
- [56] Franks GV, Djerdjev AM, Beattie JK. Absence of specific cation or anion effects at low salt concentrations on the charge at the oil/water interface. *Langmuir* 2005;21:8670–4.
- [57] Sherwood JD. Electrophoresis of gas bubbles in a rotating fluid. *J Fluid Mech* 1986;162:129–37.
- [58] Gray-Weale A, Beattie JK. An explanation for the charge on water's surface. *Phys Chem Chem Phys* 2009;11:10994–1005.
- [59] Mori Y, Young YN. From electrodiffusion theory to the electrohydrodynamics of leaky dielectrics through the weak electrolyte limit. *J Fluid Mech* 2018;855:67–130.
- [60] Kostuchenko ZA, Cui JZ, Lemay SG. Electrochemistry in micro- and nanochannels controlled by streaming potentials. *J Phys Chem C* 2020;124:2656–63.
- [61] Manciu M, Manciu FS, Ruckenstein E. On the surface tension and Zeta potential of electrolyte solutions. *Adv Colloid Interface Sci* 2017;244:90–9.
- [62] Masliyah JH, Bhattacharjee S. Electrokinetic and colloid transport phenomena. New Jersey: John Wiley & Sons; 2006.